

Supplementary Information for

Ocean currents and herbivory drive macroalgae-to-coral community shift under climate warming

Naoki H. Kumagai, Jorge García Molinos, Hiroya Yamano, Shintaro Takao, Masahiko Fujii, Yasuhiro Yamanaka

Naoki H. Kumagai
Email: nh.kuma@gmail.com

This PDF file includes:

- Supplementary text
- Figs. S1 to S8
- Tables S1 to S3
- Captions for database S1
- References for SI reference citations

Other supplementary materials for this manuscript include the following:

- Datasets S1

SI Methods

Environmental variables. We used bias-corrected (1, 2) monthly mean SST for 1950–2035 extracted from the historical (1950–2005) and projected (2006–2035) simulations of the MIROC4h model (3). Though projections for this model are only supplied until 2035 for the Representative Concentration Pathway (RCP) 4.5, it offers the highest horizontal resolution ($0.28125^\circ \times 0.1875^\circ$) for oceanic components amongst all the Coupled Model Intercomparison Project phase 5 (CMIP5) models (4)

(<https://pcmdi.llnl.gov/search/cmip5/>). To correct Miroc4h biases, we used observed monthly data (1986–2005) of the Optimum Interpolation SST version 2 (5) (provided by the National Oceanic and Atmospheric Administration ESRL PSD;

<http://www.esrl.noaa.gov/psd/>). The model biases were corrected by adding the difference in monthly climatology (1986–2005) from the observed to the modeled SST (1, 2, 6). The bias-corrected SSTs are in good agreement with those of observed SSTs in Japanese waters (6) (Fig. S6) because the MIROC4h is eddy permitting and has been developed to minimize model-data misfits in Japanese waters (3).

Daily surface current speeds (1985–2015; $0.1^\circ \times 0.1^\circ$) were sourced from the MOVE/MRI.COM ocean data assimilation system (7), which is supplied as longitudinal and latitudinal current speeds (provided by the North-East Asian Regional Global Ocean Observing System: <http://near-goos1.jodc.go.jp/>). We took monthly-median values instead of mean values to avoid bias introduced by extreme daily values. These were calculated using annual monthly data for macroalgae, given their dispersion by drifting or floating span throughout the year in Japan (8), and values from June to August in corals and herbivorous fishes, corresponding to the season when these species disperse as eggs or larvae in temperate waters around Japan (9–11). Though ocean current data go back only to 1985, directional spatial patterns remain largely stationary over time (Fig. S7).

Range centroid shifts. Centroid shifts were estimated using multi-response linear models, modeling species' location (longitude and latitude) as a function of time for each s study species ($s = 1-45$; Table S1). We reduced the spatial biases by aggregating records onto a consistent 0.05° spatial grid for each decade. Coral data from latitudes lower than 27°N was excluded because the historical and current data were not comparable. We assumed that the location $z_{i,j,s}$ of any presence record i along the Japanese coast j ($j = 1$: western; $j = 2$: eastern), is a vector of longitude $x_{i,j,s}$, and latitude $y_{i,j,s}$ that follows a multivariate normal distribution (MVN) incorporating a covariance Σ_s between longitudinal and latitudinal changes:

$$z_{i,j,s} \sim \text{MVN}(A_{j,s} + B_{j,s} \cdot t_i, \Sigma_s), \quad [1]$$

where t_i indicates decade. $A_{j,s}$ and $B_{j,s}$ are respectively vectors of intercept and coefficient comprising longitudinal and latitudinal components to be estimated for each coast. Parameters were estimated using Bayesian inference in WinBUGS 1.4.3 (12) specifying nearly non-informative normal prior distributions for coefficients, and Wishart distribution for the error term We obtained 500 estimates per parameter from 70,000

MCMC iterations after a 20,000-iteration burn-in by thinning at intervals of 100, using three chains. Convergence was verified by checking that the R-hat values ranged between 1 and 1.01 (13). Finally, we converted the coefficients (latitude/longitude) to geographic distance scale (km).

Range edge shifts. We targeted the search for range edge shifts according to the specific biogeographical situation of each species. Among the study species, three macroalgae, nine coral species and two herbivorous fishes ranged beyond Japanese territorial waters at one of their southern or northern limits, in which case only shifts for the edge defined within the study area were analyzed (Table S3). Shifts were accepted if either (i) they were directly documented in the literature (i.e., starting location, year, and duration), or else (ii) they could be directly estimated from actual occurrence records representing different periods separated by more than five years (Dataset S1). Negative and null responses were included in the analysis as our focus is on general response to climate change for the study species.

Upon detection of a range expansion or contraction, we calculated the least-cost distance (LCD) between the historical and present target cells using a 0.05° rasterized coastline to build the transition matrix. Contrary to range centroids that represent the center of mass of a distribution (i.e., can be located on land), LCDs can be reliably calculated for expansion and contractions thus reflecting shift distances more realistically than geographical distances, particularly for coastal species. We assigned a very high cost to non-coastal maritime cells to guarantee distances were calculated along the coast line except for points located on different islands. Calculations were performed with the ‘costDistance’ function of the ‘gdistance’ R package (14).

Selection of appropriate temperature predictor variables. Climate velocities, giving the rate and direction that each species would need to move to stay at the same temperature between periods, were based on different temperature parameters. Under the simplest expectation, we would expect species’ ranges to shift according to the displacement of isotherms corresponding to the initial temperatures at the locations of their historical edges, based on minimum, mean and maximum monthly SST for, respectively, leading-edge expansions, range centroid shifts and trailing-edge contractions. However, evidence suggests that there is no single temperature parameter better suited for predicting the geographic boundaries (15) of a study species, as this is very much a species-specific relationship related to factors such as survival, growth, reproduction and life cycle phase (6, 15, 16). Therefore, and because the appropriate temperature parameter that determines geographic boundaries (leading and trailing edges) is unknown for most of the study species (6, 17), we used instead a purely statistical approach.

For the centroid shifts, we calculated climate velocities for the observed occurrence points around centers of distribution, of which mean SST were within the 50% quantile, to restrict the points that are expected to follow the shifts of mean SST (i.e., not involving range edges that are expected to follow min/max SST). For the edge shifts, we first calculated climate velocities based on all SST indices: minimum (absolute minimum together with the 10% and 25% quantiles) and mean annual SSTs for the leading-edge shifts; maximum (absolute maximum, 90% and 75% quantiles) and mean annual SSTs for the trailing-edge shifts, from the annual coldest and warmest months for each year in

the series, respectively (18). Second, we selected the optimum SST index for each species and edge based on its Bayesian posterior probability (see Statistical analysis and prediction in Methods). The optimum SST indices are shown in Table S3.

Conductance matrices of thermal gradients and current speeds. To model a species range shift tracking its thermal niche under ocean warming conditions, we needed to determine temperature conductance. For a species' range shifting from warmer to cooler temperature, the value of the conductance can be calculated as the difference of temperature between the neighboring cells. Thus, the transition matrix of temperature conductance C_{sst} is defined as follows:

$$C_{sst} = SST_{focal} - SST_{neighbor}. \quad [2]$$

Here, C_{sst} is the difference between each focal cell and each of its eight neighbors, and therefore this equation represents anisotropic patterns (i.e., the friction from cell i to j is unequal to the friction from j). This conductance takes the largest value for the thermal gradient from warmer to cooler temperature within the shortest distance. To avoid negative values, the conductance was offset by adding absolute value of the minimum conductance only for cells with values.

Second, to account for the role of ocean currents in altering range shift responses to climate change, we modeled a combined conductance matrix accounting for both the spatial gradient in temperature and the speed and direction of ocean currents in each cell. The conductance ($C_{current}$) associated to moving from a focal cell i to a target cell j in a 3×3 neighborhood was calculated from the longitudinal (V_x) and latitudinal (V_y) current components at the focal cell (Fig. S8). Horizontal and vertical transitions coincident with the direction of the current components (positive values for eastward/northward and negative values for westward/southward current), were set to their absolute value, to avoid negative conductance, while the corresponding diagonal transition was calculated by the sum of the projected component values multiplied by $\cos(\pi/4)$. The conductance for the remaining 5 transitions was set to 0. The resulting conductance matrix modeled thus anisotropic mobility, i.e., a strong eastward component will result in high conductance for an eastward transition but low conductance for a westward movement.

The two resulting conductance matrices were then combined into a single conductance matrix after scaling their values (14):

$$C_{sst_current} = (1 - w) \cdot C_{sst} + w \cdot C_{current}, \quad [3]$$

where w represents the relative weight of ocean current against thermal gradient. We calculated $C_{sst_current}$ with different values of w from 0 to 1 at 0.001 interval (i.e., 1,001 calculations). All resulting conductance matrices were corrected to account for diagonal neighbors and map distortion introduced by the geographic projection before adding them together into our seascape conductance model.

SI Results

Traditional statistics for model comparison. Our results based on Bayesian inference on the relative weight of ocean currents on the prediction of the climate-driven observed range shifts, as described in the main text (Fig. 3A–C), were consistent with those resulting from using traditional statistics as the regression slopes of standardized coefficients and R^2 values associated to the individual models. The slopes of the optimized coupled climate-current model and of the current model were larger than those of the climate model, particularly in corals and herbivorous fishes (Fig. S4A–F). The optimized coupled model significantly increased the proportion of explained variance in shift response by 8.1%, 19.0% and 6.2% for range centroids, expansions and contractions, respectively, over that of the climate-only model (44.7%, 46.5% and 20.4% of variance explained). Differences in the standardized coefficients between the current model and the optimized coupled climate-current model were however small (Fig. S4D–F and G–I), though marginally better for the coupled model with 4.0%, 0.5% and 1.2% improvements in explained variance over the current model (48.8%, 65.0% and 25.4% of variance explained). This indicates that observed range shifts mostly follow a flow-based movement under climate warming, particularly for expansions and range centroid shifts, supporting our initial hypothesis.

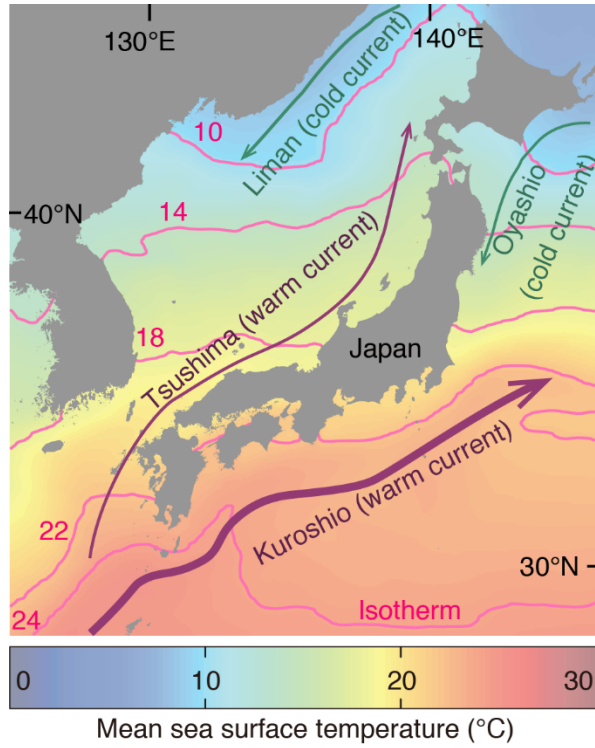


Fig. S1. A schematic of the main ocean current systems (arrows) superimposed on mean annual sea surface temperature for the 2000s. Note the different spacing and shapes of the isotherms reflecting the variability in thermal spatial gradients.

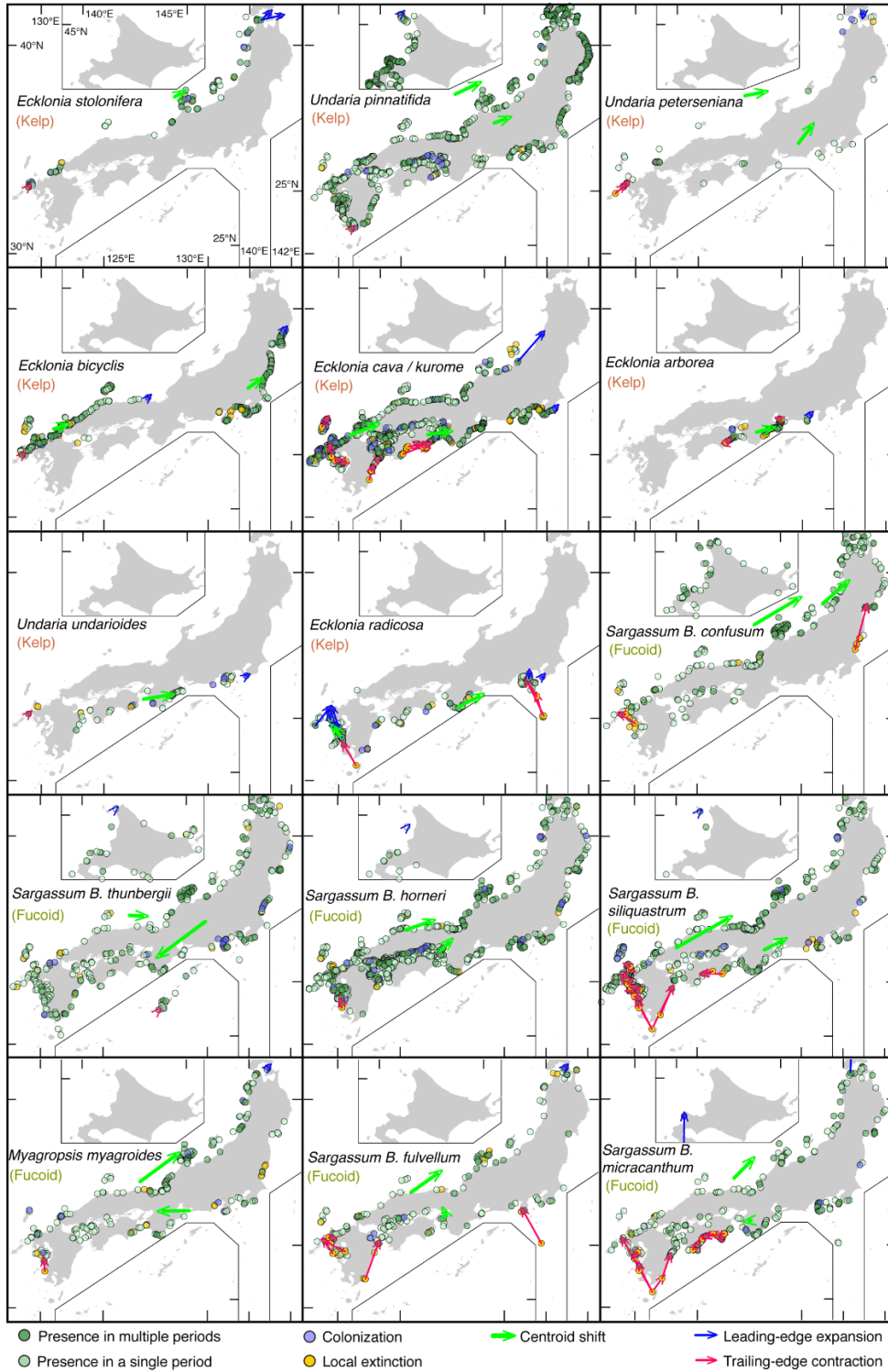


Fig. S2. Distributions and range shifts of each study species in Japan. Records mapped are presences (recorded in a single or multiple periods), colonizations, local extinctions, centroid shifts (western and eastern coasts), leading-edge expansions, and trailing-edge contractions. Each point represents 0.05° grid cell.

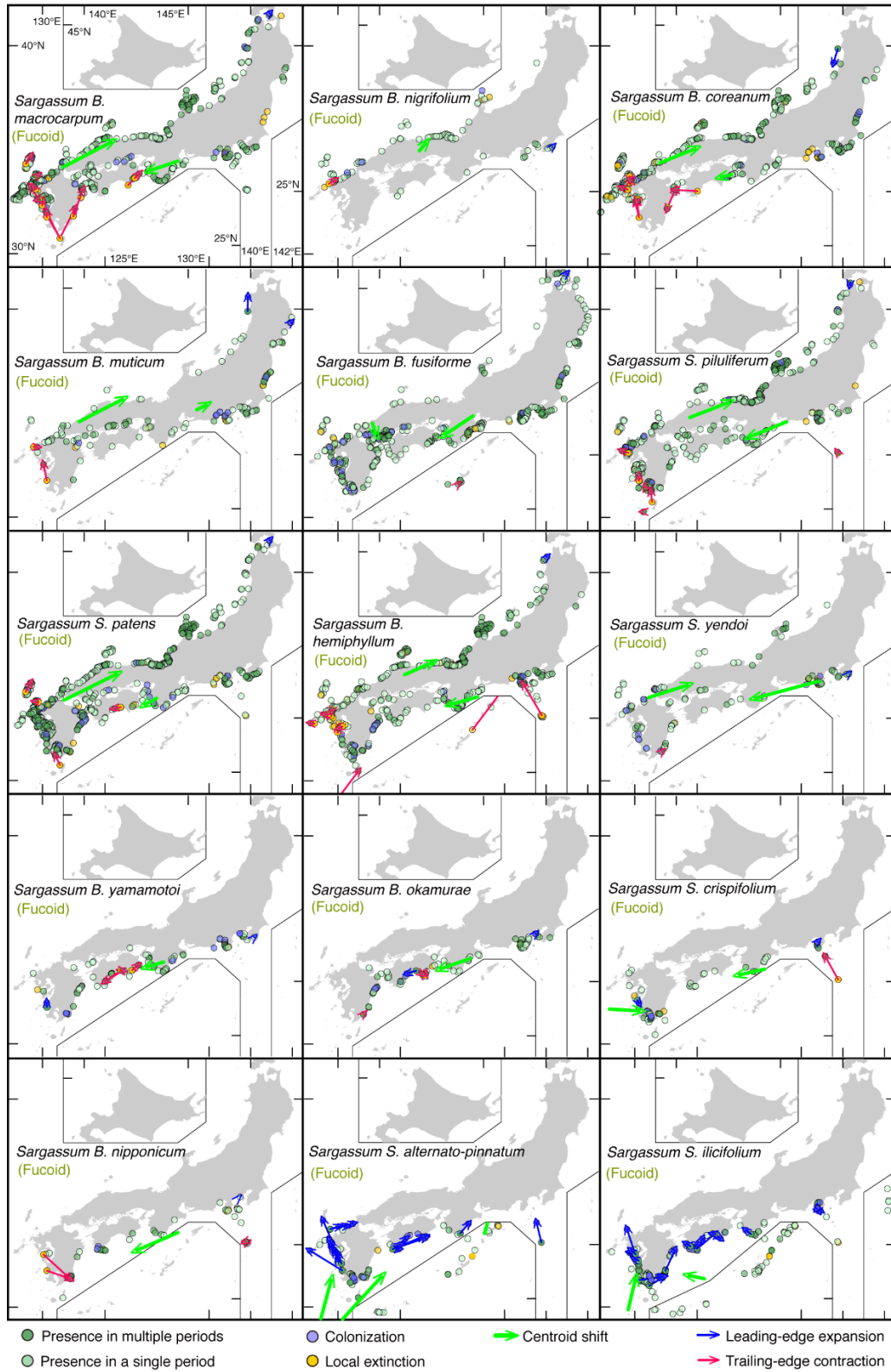


Fig. S2. (continued) Distributions and range shifts of each study species in Japan.

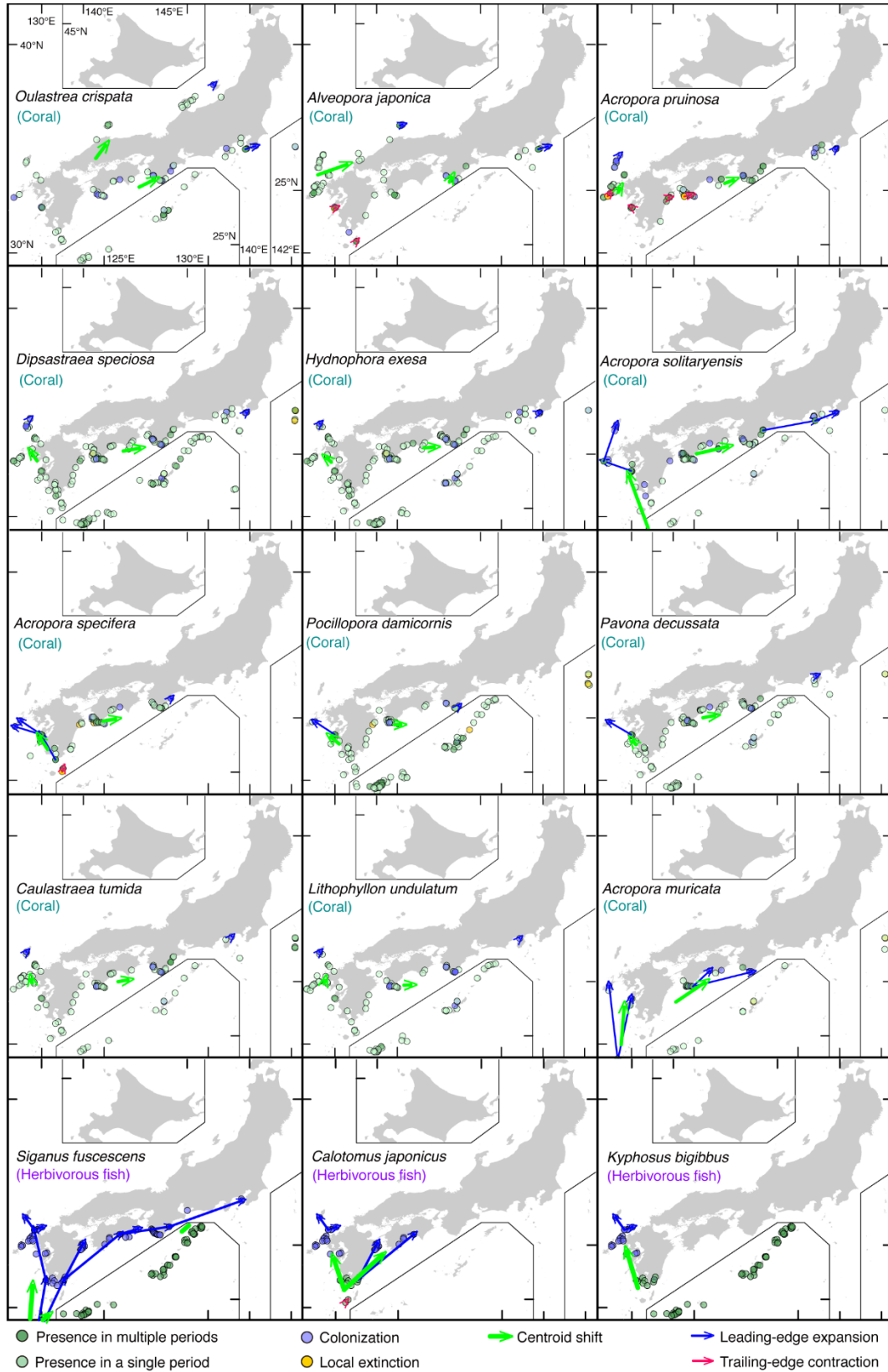


Fig. S2. (continued) Distributions and range shifts of each study species in Japan.

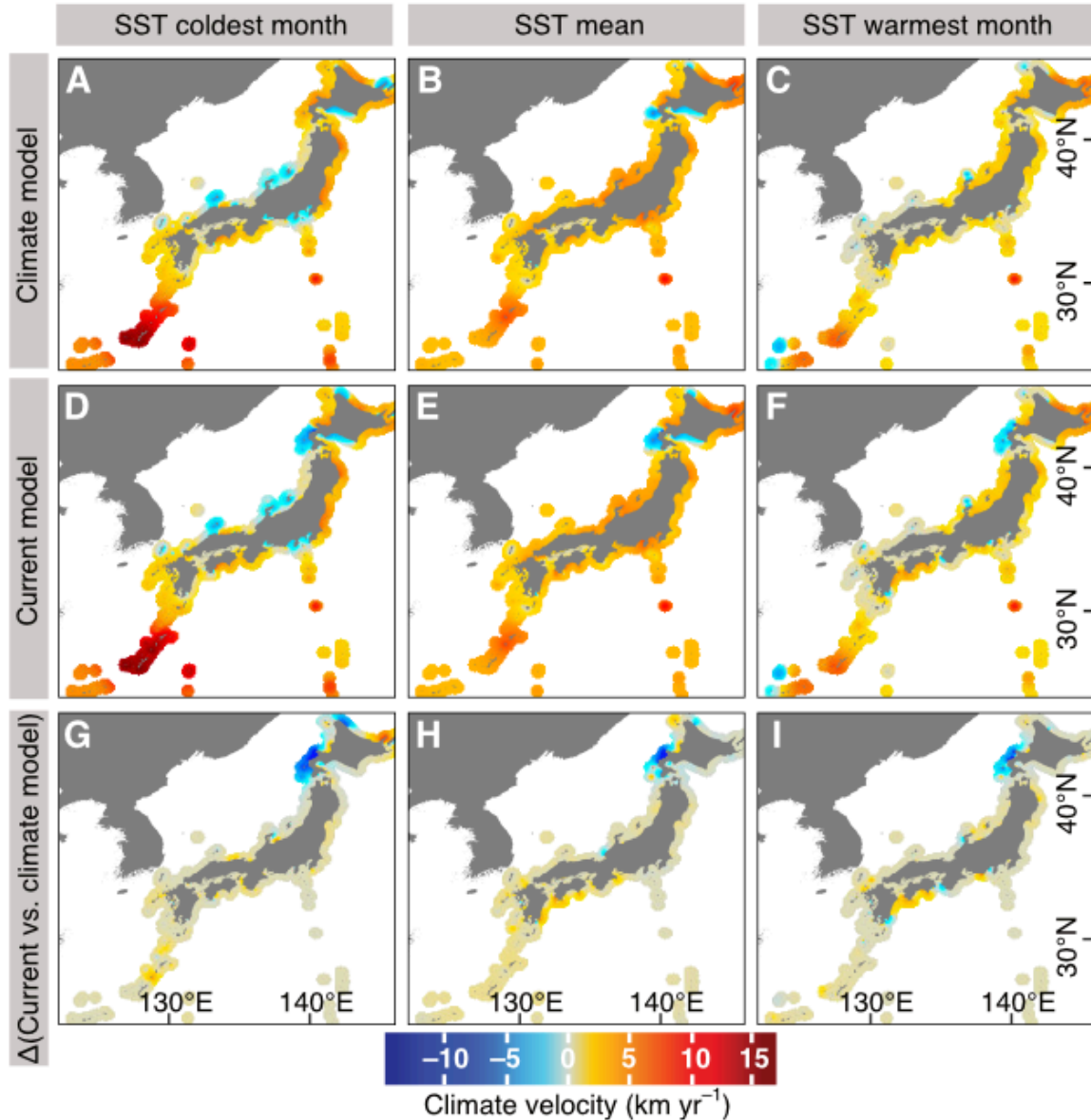


Fig. S3. Climate velocity used for prediction of range shifts. Velocity cell-estimates based on annual (*A, D, G*) minimum, (*B, E, H*) mean, and (*C, F, I*) maximum mean monthly SST (5-year means SST for 1970–2009) calculated as the least-cost path distance between each coastal focal cell and its closest cell having the same temperature in 2009 as the focal cell had in 1970, divided by 40 years. Least-cost path distances were calculated using either (*A–C*) a climate prediction of least-cost path model accounting only for the effect of climate or (*D–F*) a current model (see Fig. 1C), and (*G–I*) the differences between the estimates of the two models are depicted. Calculations of velocity were restricted to coastal grids, since the study species inhabit coastal environments. Figures were spatially interpolated to 50 km from the coast using inverse distance weighted method to aid visualization.

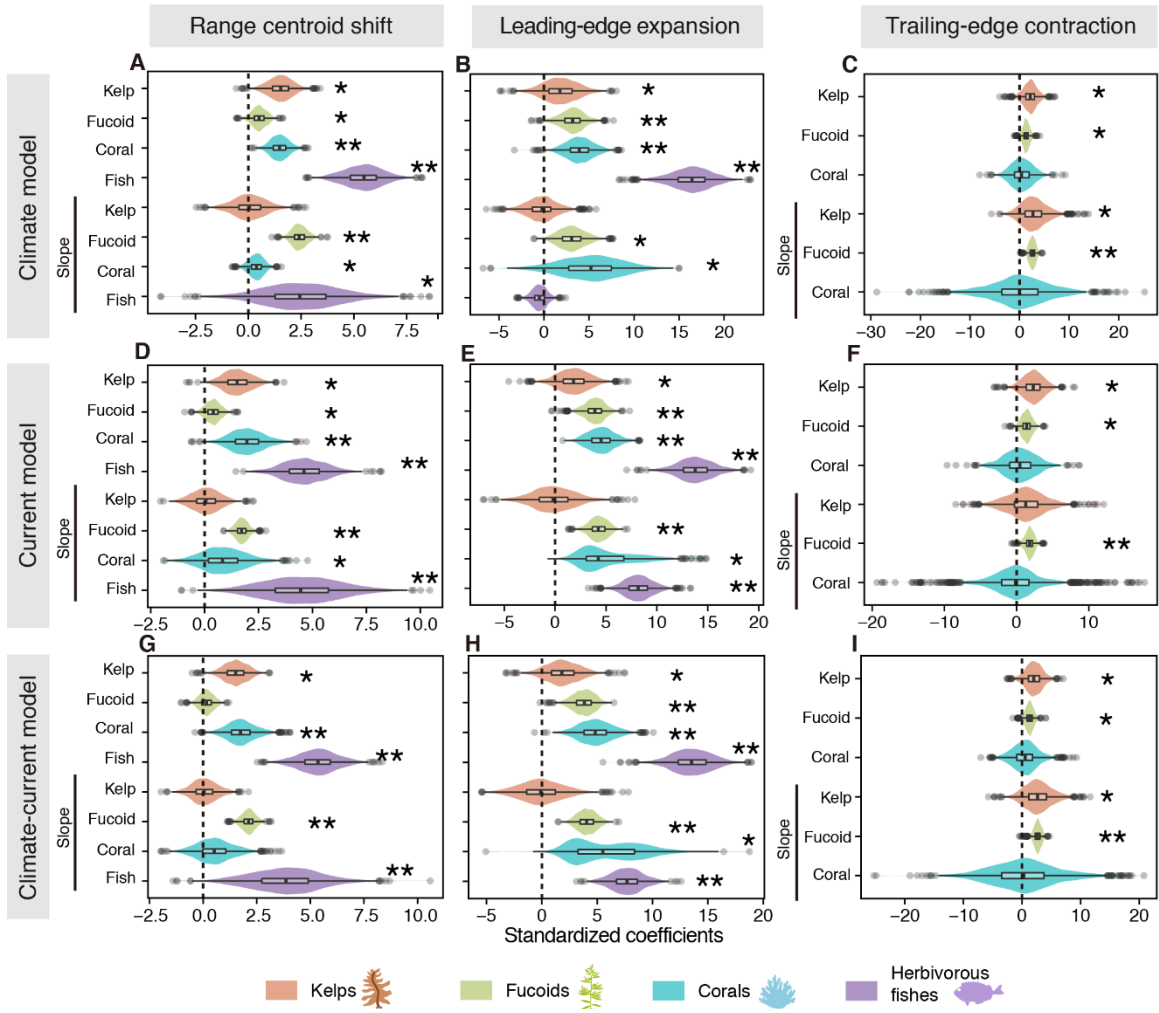


Fig. S4. Bayesian posterior distributions of standardized coefficients in predicted shift rates for (A, D, G) the range centroid shift, (B, E, H) leading-edge expansion, and (C, F, I) trailing-edge contraction for (A–C) climate models, (D–F) current models or (G–I) optimized coupled climate and current models. Violin plot summarizes posterior distributions with box-and-whisker plot showing the median (vertical line inside the box), 50% (box) and 95% (whiskers) credible intervals (CI), and outliers (dots). **: 95% CI does not overlap 0; *: 50% CI does not overlap 0.

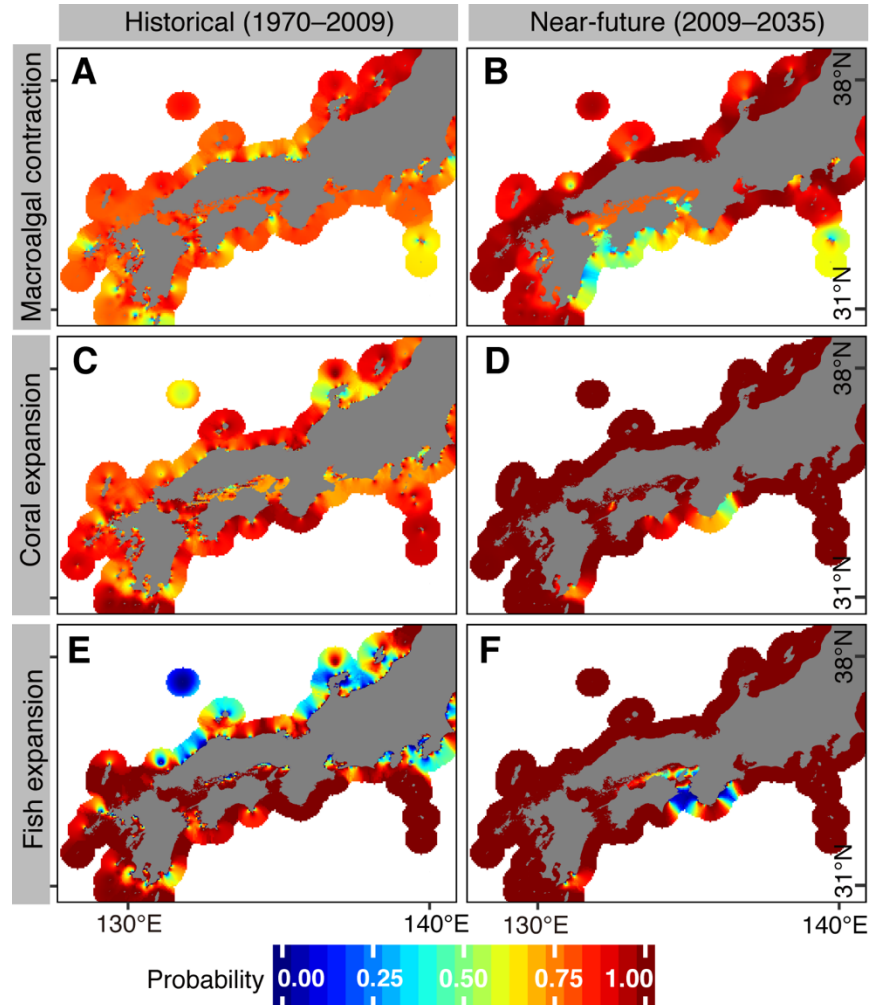


Fig. S5. Estimated cell-based probability of potential range shifts based on predicted rates of taxa's shifts. (A, B) Range contraction of macroalgae, (C, D) range expansion of corals, (E, F) range expansion of herbivorous fishes. Predictions based on (A, C, E) historical (1970–2009) and (B, D, F) near-future (2009–2035) climatic conditions. Inset histograms represent frequency distributions of probabilities with respective mean values. Probabilities of shifts were obtained from the Bayesian posterior distributions of predicted shift rates based on the coupled climate-current model. Calculations were restricted to coastal grids, since the study species inhabit coastal environments. Values are spatially interpolated to 50 km from the coast using the inverse distance weighted method to aid visualization.

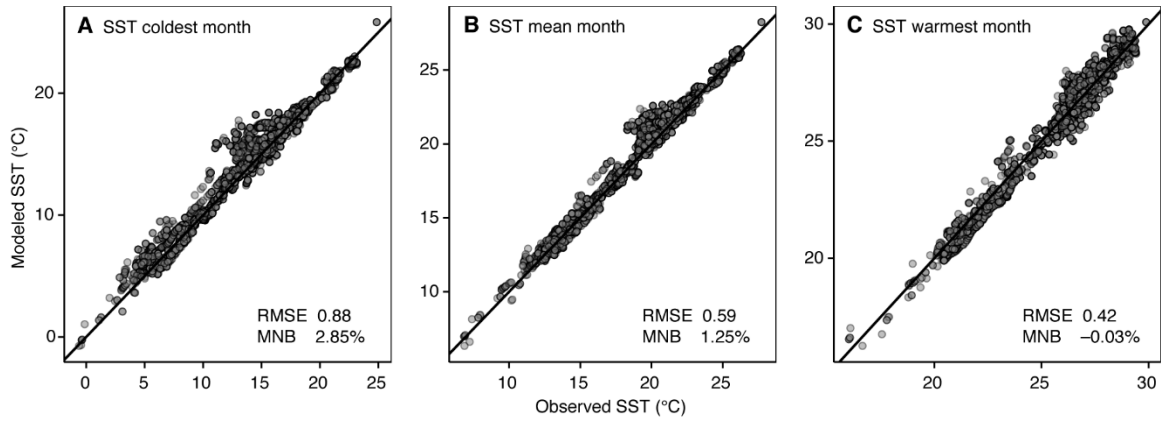


Fig. S6. Comparisons of (A) coldest, (B) mean and (C) warmest observed (OISST) and modeled (MIROC4h) monthly SSTs during 1982–2015 at the all species occurrence points. The solid line indicates the 1:1 line.

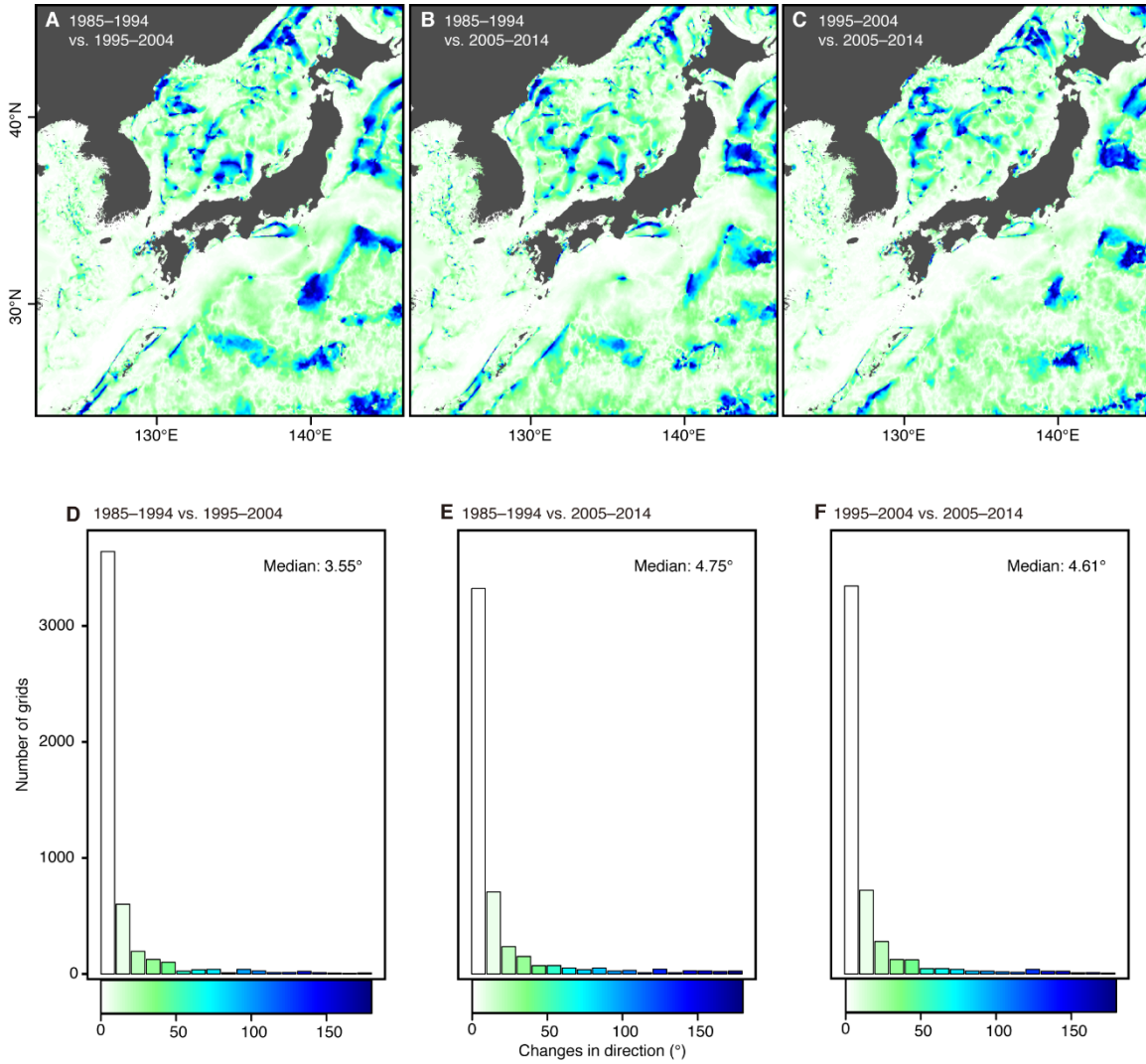


Fig. S7. Temporal changes in median direction of ocean current (surface currents, MOVE/MRI.COM). (A, D), 1985–1994 vs. 1995–2004. (B, E), 1985–1994 vs. 2005–2014. (C, F), 1995–2004 vs. 2005–2014. (D, F) Frequency distribution of the changes in current direction between periods at all the grids covering species presence data used in this study.

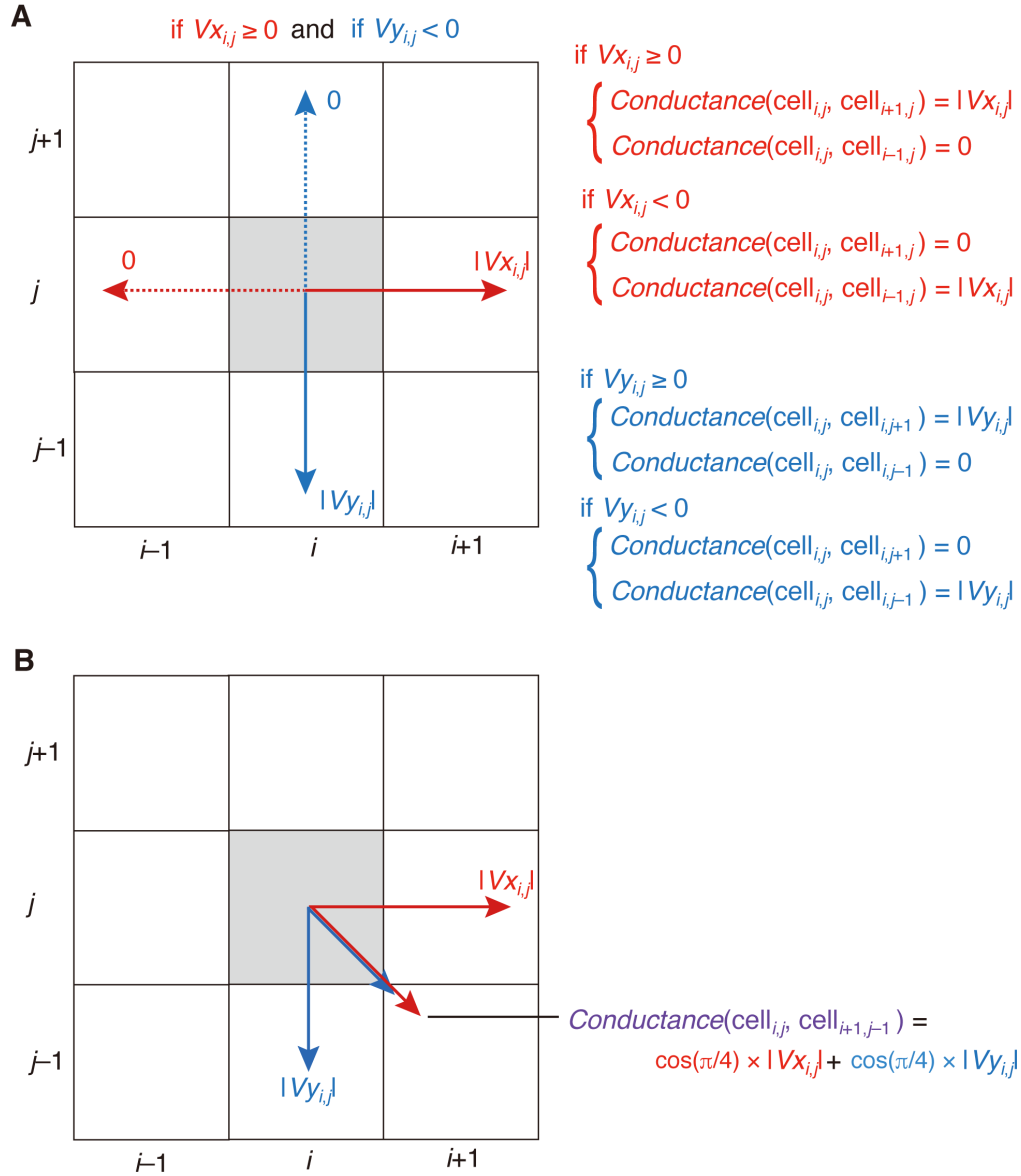


Fig. S8. Definition of the conductance values associated to moving from a focal cell i,j to each of its 8 neighboring cells following ocean current transport. $\text{Conductance}(\text{cell}_{\text{focal}}, \text{cell}_{\text{target}})$ represents conductance for a transition from the focal cell ‘cell_{focal}’ to target cell ‘cell_{target}’. $Vx_{i,j}$ and $Vy_{i,j}$ are longitudinal and latitudinal components of ocean current velocity at focal the cell ‘cell_{*i,j*}’. The source data (MOVE/MRI.COM, see **SI Methods**) have positive values for eastward/northward and negative values for westward/southward current. (A) The conductance for a transition from a focal cell to its horizontal/vertical neighbors matching the two current velocity components is equal to their absolute value to avoid negative conductance, while the that for the remaining target neighbors is 0. (B) Conductance for diagonal transitions was estimated in a similar way, the diagonal component matching the focal current direction calculated as the sum of the projections of the vertical and horizontal current components into the diagonal axis.

Table S1. Descriptions of the study species. These species are ordered from northernmost to southernmost distribution. Scientific name has been checked using AlgaeBase (19) for macroalgae, WoRMS (20) for corals and FishBase (21) for fishes. Although the study macroalgal species consist of only four genera, they comprise the main habitat-forming species along the rocky marine coasts of the Japanese temperate zone (22, 23). Among the genus *Sargassum*, those belonging to subgenus *Bactrophyucus* distributes temperate zone while subgenus *Sargassum* are regarded as tropical species, because the subgenus distributes mainly the tropical zone (22) and are typically short-lived and rapidly-regenerating species (24).

Species	Order	Family	Subgenus	Synonym	Notes
Macroalgae (kelps)					
<i>Ecklonia stolonifera</i>	Laminariales	Lessoniaceae			
<i>Undaria pinnatifida</i>	Laminariales	Alariaceae		<i>Alaria pinnatifida</i>	
				<i>Undaria pinnatifida</i> var.	
				<i>distans</i>	
				<i>Undaria pinnatifida</i> f.	
				<i>narutensis</i>	
				<i>Undaria pinnatifida</i> f.	
				<i>subflabellata</i>	

U. peterseniana Laminariales Alariaceae

E. bicyclis Laminariales Lessoniaceae

E. cava/kurome Laminariales Lessoniaceae

Eisenia bicyclis

Ecklonia kurome

We regarded *E. kurome* as a synonym as in (23), because of the morphological and genetic overlaps with *E. cava*

E. arborea Laminariales Lessoniaceae

Eisenia arborea

U. undarioides Laminariales Alariaceae

Hirome undarioides

E. radicata Laminariales Lessoniaceae

Eckloniopsis radicata

Macroalgae (fucooids)

Sargassum confusum Fucales Sargassaceae *Bactrophycus*

S. thunbergii Fucales Sargassaceae *Bactrophycus*

S. horneri Fucales Sargassaceae *Bactrophycus* *Sargassum filicinum*

S. siliquastrum Fucales Sargassaceae *Bactrophycus*

<i>Myagropsis myagroides</i>	Fucales	Sargassaceae		<i>Cystoseira sisymbrioides</i> <i>Cystophyllum caespitosum</i> <i>Cystophyllum sisymbroides</i> <i>Myagropsis yendoi</i>
<i>S. fulvellum</i>	Fucales	Sargassaceae	<i>Bactrophyucus</i>	
<i>S. micracanthum</i>	Fucales	Sargassaceae	<i>Bactrophyucus</i>	
<i>S. macrocarpum</i>	Fucales	Sargassaceae	<i>Bactrophyucus</i>	<i>S. tortile f. macrocarpum</i>
<i>S. nigrifolium</i>	Fucales	Sargassaceae	<i>Bactrophyucus</i>	
<i>S. coreanum</i>	Fucales	Sargassaceae	<i>Bactrophyucus</i>	<i>S. ringgoldianum</i> ssp. <i>coreanum</i>
<i>S. muticum</i>	Fucales	Sargassaceae	<i>Bactrophyucus</i>	<i>S. kjellmanianum f.</i> <i>muticum</i>
<i>S. fusiforme</i>	Fucales	Sargassaceae	<i>Bactrophyucus</i>	<i>Hizikia fusiformis</i>
<i>S. patens</i>	Fucales	Sargassaceae	<i>Sargassum</i>	<i>S. Schizophycus patens</i>
<i>S. piluliferum</i>	Fucales	Sargassaceae	<i>Sargassum</i>	<i>S. Phyllotrichia piluliferum</i>

<i>S. hemiphyllum</i>	Fucales	Sargassaceae	<i>Bactrophyucus</i>	
<i>S. yendoi</i>	Fucales	Sargassaceae	<i>Sargassum</i>	
<i>S. yamamotoi</i>	Fucales	Sargassaceae	<i>Bactrophyucus</i>	
<i>S. okamurae</i>	Fucales	Sargassaceae	<i>Bactrophyucus</i>	
<i>S. nipponicum</i>	Fucales	Sargassaceae	<i>Bactrophyucus</i>	
<i>S. crispifolium</i>	Fucales	Sargassaceae	<i>Sargassum</i>	
<i>S. alternato-pinnatum</i>	Fucales	Sargassaceae	<i>Sargassum</i>	<i>S. asymmetricum</i>
<i>S. ilicifolium</i>	Fucales	Sargassaceae	<i>Sargassum</i>	<i>S. ilicifolium</i> var. <i>conduplicatum</i> <i>S. duplicatum</i> <i>S. brevifolium</i> <i>S. cristaefolium</i>

Corals

<i>Oulastrea crispata</i>	Scleractinia	Scleractinia incertae sedis
---------------------------	--------------	--------------------------------

<i>Alveopora japonica</i>	Scleractinia	Acroporidae	
<i>Acropora pruinosa</i>	Scleractinia	Acroporidae	<i>Ac. pruinosa/tumida</i> in (25)
<i>Dipsastraea speciosa</i>	Scleractinia	Merulinidae	<i>Favia speciosa</i> <i>Favia speciosa</i> in (25), genus revised
<i>Hydnophora exesa</i>	Scleractinia	Merulinidae	
<i>Ac. solitaryensis</i>	Scleractinia	Acroporidae	
<i>Ac. spicifera</i>	Scleractinia	Acroporidae	<i>Ac. hyacinthus</i> in (25), but the northern populations turned to be <i>Ac. spicifera</i>
<i>Pocillopora</i>			
<i>damicornis</i>	Scleractinia	Pocilloporidae	
<i>Pavona decussata</i>	Scleractinia	Agariciidae	
<i>Caulastraea tumida</i>	Scleractinia	Merulinidae	
<i>Lithophyllon</i>			
<i>undulatum</i>	Scleractinia	Fungiidae	

Table S2. Summary of range shift rates (km year⁻¹) grouped by taxa and type of shift. Figures refer to the mean shift rate \pm 1 standard deviation, and the percentages of poleward shifts, zero responses, and equatorward shifts. See Dataset S1 for shift rate of each species and analysis.

	Range centroid shifts	Leading-edge expansions	Trailing-edge contractions
Total	1.32 \pm 2.70 (78.5%)	5.60 \pm 8.44 (62.1 / 30.2 / 7.8%)	1.61 \pm 4.10 (68.9 / 9.6 / 21.5%)
Kelps	1.51 \pm 0.59 (100%)	1.72 \pm 2.40 (57.9 / 36.8 / 5.3%)	2.39 \pm 2.88 (75.0 / 16.7 / 8.3%)
Fucoids	0.87 \pm 3.30 (57.5%)	3.91 \pm 6.18 (56.6 / 28.3 / 15.1%)	1.53 \pm 4.47 (68.0 / 5.8 / 26.2%)
Corals	1.47 \pm 1.35 (100%)	4.20 \pm 5.43 (51.7 / 48.3 / 0.0%)	0.42 \pm 0.33 (71.4 / 28.6 / 0.0%)
Fishes	5.30 \pm 2.89 (100%)	18.21 \pm 12.32 (100 / 0.0 / 0.0%)	0.00 \pm 0.00 (0.0 / 100 / 0.0%)

Table S3. Indices of sea surface temperature (SST) for each species and each edge. The Bayesian posterior probability of index to be selected are shown for each species and each edge to rank SST indices. The index with the maximum probability is shown in bold face for each species and edge. Max: annual maximum of monthly mean; Q10%, Q25%, Q75%, Q90%: 10%, 25%, 75%, 90% quantile of monthly mean, respectively; Min: annual minimum of monthly mean. Dash: the edge is outside of Japanese territorial waters, or not included in the index selection (because only one stationary trailing-edge for herbivorous fishes).

Species	Leading-edge expansions				Trailing-edge contractions			
	Min	Q10%	Q25%	Mean	Min	Q10%	Q25%	Mean
Macroalgae (kelps)								
<i>Ecklonia stolonifera</i>	0.270	0.263	0.191	0.275	0.116	0.261	0.308	0.315
<i>Undaria pinnatifida</i>	0.250	0.237	0.253	0.260	0.272	0.253	0.230	0.245
<i>U. peterseniana</i>	0.237	0.265	0.245	0.253	0.260	0.230	0.259	0.251
<i>E. bicyclis</i>	0.256	0.244	0.245	0.255	0.252	0.250	0.247	0.251
<i>E. cava/kurome</i>	0.264	0.243	0.235	0.258	0.209	0.296	0.253	0.243
<i>E. arborea</i>	0.269	0.266	0.239	0.225	0.231	0.259	0.265	0.244
<i>U. undarioides</i>	0.233	0.262	0.231	0.274	0.251	0.239	0.251	0.260
<i>E. radicata</i>	0.238	0.260	0.247	0.255	0.173	0.215	0.297	0.315
Macroalgae (fucoioids)								
<i>Sargassum confusum</i>	0.243	0.259	0.252	0.246	0.894	0.033	0.068	0.005
<i>S. thunbergii</i>	0.223	0.251	0.257	0.269	0.223	0.012	0.386	0.379
<i>S. horneri</i>	0.253	0.164	0.251	0.332	0.219	0.250	0.274	0.257
<i>S. siliquastrum</i>	0.256	0.261	0.227	0.256	0.492	0.167	0.154	0.187
<i>Myagropsis myagroides</i>	0.235	0.248	0.250	0.267	0.250	0.245	0.267	0.238
<i>S. fulvellum</i>	0.259	0.237	0.244	0.260	0.103	0.249	0.280	0.369

<i>S. micracanthum</i>	0.407	0.069	0.091	0.434	0.003	0.165	0.340	0.493
<i>S. macrocarpum</i>	0.251	0.254	0.253	0.242	0.337	0.269	0.185	0.209
<i>S. nigrifolium</i>	0.260	0.277	0.230	0.233	0.255	0.256	0.255	0.234
<i>S. coreanum</i>	0.223	0.241	0.262	0.273	0.125	0.203	0.345	0.327
<i>S. muticum</i>	0.373	0.287	0.183	0.157	0.217	0.227	0.300	0.257
<i>S. fusiforme</i>	0.273	0.237	0.236	0.254	0.040	0.947	0.005	0.008
<i>S. piluliferum</i>	0.271	0.223	0.215	0.291	0.140	0.254	0.223	0.383
<i>S. patens</i>	0.207	0.273	0.256	0.264	0.321	0.179	0.134	0.366
<i>S. hemiphyllum</i>	0.271	0.248	0.231	0.250	0.931	0.030	0.013	0.026
<i>S. yendoi</i>	0.251	0.252	0.261	0.235	0.255	0.241	0.255	0.248
<i>S. yamamotoi</i>	0.288	0.256	0.206	0.250	0.379	0.325	0.173	0.123
<i>S. okamurae</i>	0.002	0.657	0.177	0.164	0.395	0.212	0.204	0.189
<i>S. crispifolium</i>	0.277	0.250	0.243	0.230	0.275	0.251	0.214	0.260
<i>S. nipponicum</i>	0.265	0.214	0.269	0.252	0.659	0.150	0.095	0.096
<i>S. alternato-pinnatum</i>	0.275	0.143	0.218	0.364	—	—	—	—
<i>S. ilicifolium</i>	0.901	0.043	0.009	0.047	0.295	0.005	0.324	0.376
Corals								
<i>Oulastrea crispata</i>	0.264	0.267	0.233	0.235	—	—	—	—
<i>Alveopora japonica</i>	0.280	0.237	0.227	0.255	0.140	0.277	0.287	0.295
<i>Acropora pruinosa</i>	0.250	0.269	0.222	0.259	0.148	0.291	0.297	0.263
<i>Dipsastraea speciosa</i>	0.255	0.251	0.218	0.276	—	—	—	—
<i>Hydnophora exesa</i>	0.261	0.237	0.233	0.269	—	—	—	—
<i>Ac. solitaryensis</i>	0.182	0.094	0.088	0.636	—	—	—	—
<i>Ac. spicifera</i>	0.121	0.263	0.321	0.295	0.255	0.250	0.247	0.247
<i>Pocillopora damicornis</i>	0.167	0.203	0.171	0.459	—	—	—	—
<i>Pavona decussata</i>	0.170	0.157	0.155	0.519	—	—	—	—

<i>Caulastraea tumida</i>	0.255	0.263	0.225	0.256	—	—	—	—
<i>Lithophyllon undulatum</i>	0.268	0.251	0.211	0.271	—	—	—	—
<i>Ac. muricata</i>	0.201	0.201	0.203	0.395	—	—	—	—
Herbivorous fishes								
<i>Siganus fuscescens</i>	1.000	0.000	0.000	0.000	—	—	—	—
<i>Calotomus japonicus</i>	0.363	0.199	0.395	0.043	—	—	—	—
<i>Kyphosus bigibbus</i>	0.161	0.200	0.397	0.241	—	—	—	—

Dataset S1 (separate file)

Shift rate (km year^{-1}) and reference information on the contributed data set, compiled for each species and analysis. (A) Range centroid shifts for each species and decade. (B) Leading and trailing edge shifts for each species. Centroid shift rates were estimated by multi-response linear models (**SI Methods**). Records for herbivorous fishes represent deforestation of macroalgal communities due to tropical herbivorous fishes. Reference numbers for macroalgae indicate resourceID in (23), references for corals and herbivorous fishes are listed in footnote. See Fig. 2A for the division between western and eastern coasts in (A). Southern regions for data of herbivorous fishes (c.a. lower than 29°N) belong to subtropical zone and have been dominated by corals and tropical macroalgae since the oldest records. References in each parenthesis in (B) constitute an individual shift. An underlined reference in (B) indicates that the study identified the shift previously, whereas the others were identified by this study. We identified the reported geographical locations for 85% of all survey sites with an accuracy of 1 km. There were no apparent spatial or temporal gaps in survey data: at least two decades of replications were available in most locations (Fig. S2).

References

1. Tabor K, Williams JW (2010) A Globally downscaled climate projections for assessing the conservation impacts of climate change. *Ecol Appl* 20(2): 554–565
2. Yara Y, et al. (2011) Projection and uncertainty of the poleward range expansion of coral habitats in response to sea surface temperature warming: a multiple climate model study. *Galaxea* 13(1):11–20.
3. Sakamoto TT, et al. (2012) MIROC4h – a new high-resolution atmosphere–ocean coupled general circulation model. *J Meteorol Soc Jpn* 90(3):325–359.
4. Taylor KE, Stouffer RJ, Meehl GA (2012) An overview of CMIP5 and the experiment design. *Bull Am Meteorol Soc* 93:485–498.
5. Reynolds RW, et al. (2007) Daily high-resolution-blended analyses for sea surface temperature. *J Clim* 20:5473–5496.
6. Takao S, et al. (2015) An improved estimation of the poleward expansion of coral habitats based on the inter-annual variation of sea surface temperatures. *Coral Reefs* 34(4):1125–1137.
7. Usui N, et al. (2006) Meteorological Research Institute multivariate ocean variational estimation (MOVE) system: some early results. *Adv Space Res* 37(4):806–822.
8. Hirata T, et al. (2001) Ecological studies on the community of drifting seaweeds in the south-eastern coastal waters of Izu Peninsula, central Japan. I: Seasonal changes of plants in species composition, appearance, number of species and size. *Phycol Res* 49(3):215–229.

9. Mezaki T, et al. (2007) Spawning patterns of high latitude scleractinian corals from 2002 to 2006 at Nishidomari, Otsuku, Kochi, Japan. *Kuroshio Biosphere* 3:33–47.
10. Yamada H, Kiriyaama T, Yoshimura T (2006) Latitudinal differences in early life ecology of *Siganus fuscescens*. *Fish Engineer* 43(1):35–39.
11. Yamaguchi A, Kume G, Yoshimura T, Kiriyaama T, Yoshimura T (2011) Spawning season and size at sexual maturity of *Kyphosus bigibbus* (Kyphosidae) from northwest Kyushu, Japan. *Ichthyol Res* 58(3):283–287.
12. Lunn DJ, Thomas A, Best N, Spiegelhalter D (2000) WinBUGS – a Bayesian modelling framework: concepts, structure, and extensibility. *Stat Comput* 10(4):325–337.
13. Gelman A, et al. (2013) *Bayesian Data Analysis* (Chapman & Hall, New York), 3rd Ed.
14. van Etten J (2015) *gdistance: Distances and Routes on Geographical Grids*. R package version 1.1-9.
15. Breeman AM (1988) Relative importance of temperature and other factors in determining geographical boundaries of sea-weeds: experimental and phenological evidence. *Helgoland Wiss Meer* 42(2):199–241.
16. Saxby T, Dennison WC, Hoegh-Guldberg O (2003) Photosynthetic responses of the coral *Montipora digitata* to cold temperature stress. *Mar Ecol Prog Ser* 248:85–97.
17. Baba M (2014) Effects of temperature on the growth and survival of five Sargassaceous species from Niigata prefecture in laboratory culture. *Rep Mar Ecol Res Inst* 19:53–61.

18. Hiddink JG, Burrows MT, García Molinos J (2014) Temperature tracking by North Sea benthic invertebrates in response to climate change. *Glob Change Biol* 21(1):117–129.
19. Guiry MD, Guiry GM (2016) *AlgaeBase*. www.algaebase.org. Accessed Mar 3, 2017.
20. WoRMS Editorial Board (2016) *World Register of Marine Species*. www.marinespecies.org. Accessed Mar 3, 2017.
21. Froese R, Pauly D (2016) *FishBase*. www.fishbase.org. Accessed Mar 3, 2017.
22. Phillips N (1995) Biogeography of *Sargassum* (Phaeophyta) in the Pacific basin. *Taxonomy of Economic Seaweeds*, eds Abbott IA, vol. 5 (La Jolla, California: California Sea Grant College System), pp 107–145.
23. Kumagai NH, Yamano H, Fujii M, Yamanaka Y (2016) Habitat-forming seaweeds in Japan (fucoids and temperate kelps). *Ecol Res* 31(6):759–759; last update 30 Aug 2016.
24. Yatsuya K, Kiyomoto S, Yoshida G, Yoshimura T (2012) Regeneration of the holdfast in 13 species of the genus *Sargassum* grown along the western coast of Kyushu, south-western Japan. *Jpn J Phycol* 60(2):41–45.
25. Yamano H, Sugihara K, Nomura K (2011) Rapid poleward range expansion of tropical reef corals in response to rising sea surface temperatures. *Geophys Res Lett* 38(4):L04601.